JACS
JOURNAL OF THE AMERICAN CHEMICAL SOCIETY
Article
pubs.acs.org/JACS

Molecular Spintronics: Destructive Quantum Interference Controlled by a Gate

Aldilene Saraiva-Souza,*[,†] Manuel Smeu,*[,‡] Lei Zhang,[†] Antonio Gomes Souza Filho,[§] Hong Guo,[†] and Mark A. Ratner[‡]

[†]Centre for the Physics of Materials and Department of Physics, McGill University, Montreal, QC H3A 2T8, Canada
[‡]Departamento of Chemistry, Northwestern University, Evanston, Illinois 60208, United States
[§]Departamento de Física, Universidade Federal do Ceará, Fortaleza, CE 60440-900, Brazil

Supporting Information

ABSTRACT: The ability to control the spin-transport properties of a molecule bridging conducting electrodes is of paramount importance to molecular spintronics. Quantum interference can play an important role in allowing or forbidding electrons from passing through a system. In this work, the spin-transport properties of a polyacetylene chain bridging zigzag graphene nanoribbons (ZGNRs) are studied with nonequilibrium Green's function calculations performed within the density functional theory framework (NEGF-DFT). ZGNR electrodes have inherent spin polarization along their edges, which causes a splitting between the properties of spin-up and spin-down electrons in these systems. Upon adding an imidazole donor group and a pyridine acceptor group to the polyacetylene chain, this causes destructive interference features in the electron transmission spectrum. Particularly, the donor group causes a large antiresonance dip in transmission at the Fermi energy E_F of the electrodes. The application of a gate is investigated and found to provide control over the energy position of this feature making it possible to turn this phenomenon on and off. The current−voltage (I−V) characteristics of this system are also calculated, showing near ohmic scaling for spin-up but negative differential resistance (NDR) for spin-down.

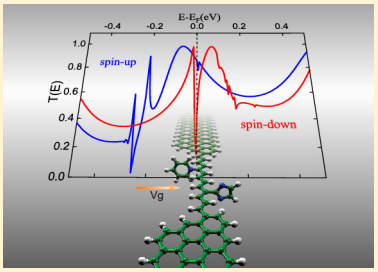

INTRODUCTION

Since it was first proposed that a single molecule might be used as a rectifier,[1] there has been a large effort aimed at designing molecular systems to perform as other basic electronic components. One of the most important goals of nanoelectronics is the ability to reversibly turn on and off the current passing through a molecular device, as in a transistor. Promising studies in this area have combined the properties of molecular electronics with those of spintronics, which are commonly investigated in nonmagnetic systems coupled to electrodes possessing magnetic properties.[2] This typically involves an organic molecule connected to metal electrodes, but it has been suggested that the physical connection between the two is not well-suited to electron transport.[3−6] The bridging of single-walled carbon nanotubes (CNTs) with molecules was achieved experimentally a few years ago.[7] However, these yield low conductance values due to the difficulty in creating covalent contacts and because the contact transparency is highly dependent on the nature of the connection between the molecule and the CNT.[8] On the other hand, experimental results have shown that a single layer of graphene might make an ideal metallic electrode and may improve the ability of molecules to function as devices.[9,10] Very recently, the fabrication of perfect graphene nanoribbons has brought such electronic devices to reality.[11] In particular, zigzag graphene nanoribbons (ZGNRs) have shown striking magnetic properties based on their spin polarization along their edges.[12] The half-metallicity behavior under a gate voltage might offer a major advance toward creating organic devices.[12,13]

There are advantages of the carbon nanoribbon structure beyond its magnetic properties. For instance, a carbon chain coupled between ZGNRs is stable in several different configurations[14,15] and can be a very efficient spin filter device that can be switched on and off.[16] The tunability of *trans*-polyacetylene has been demonstrated in work showing that its geometry and electronic structure are affected by the presence of an electric field.[17] The ability to control electron transport through the molecule is essential in nanoscale devices, and there is particular interest in systems in which it is possible to switch the conductance between on and off states. One effective method for achieving such control may be by exploiting constructive and destructive quantum interference effects.[18] This phenomenon has been extensively discussed for benzene rings, where the relative positions of anchoring groups (para or meta) will determine the interference pathways through the molecular ring.[19−22] Typically, the meta connection results in an antiresonance peak close to the Fermi energy E_F of the electrodes, which indicates destructive quantum interference (DQI), resulting in low conductance (off state). The first experimental observation of DQI was obtained indirectly from mechanically controlled break junctions, measuring ultralow

Received: August 19, 2014
Published: September 29, 2014

   dx.doi.org/10.1021/ja508537n | J. Am. Chem. Soc. 2014, 136, 15065−15071

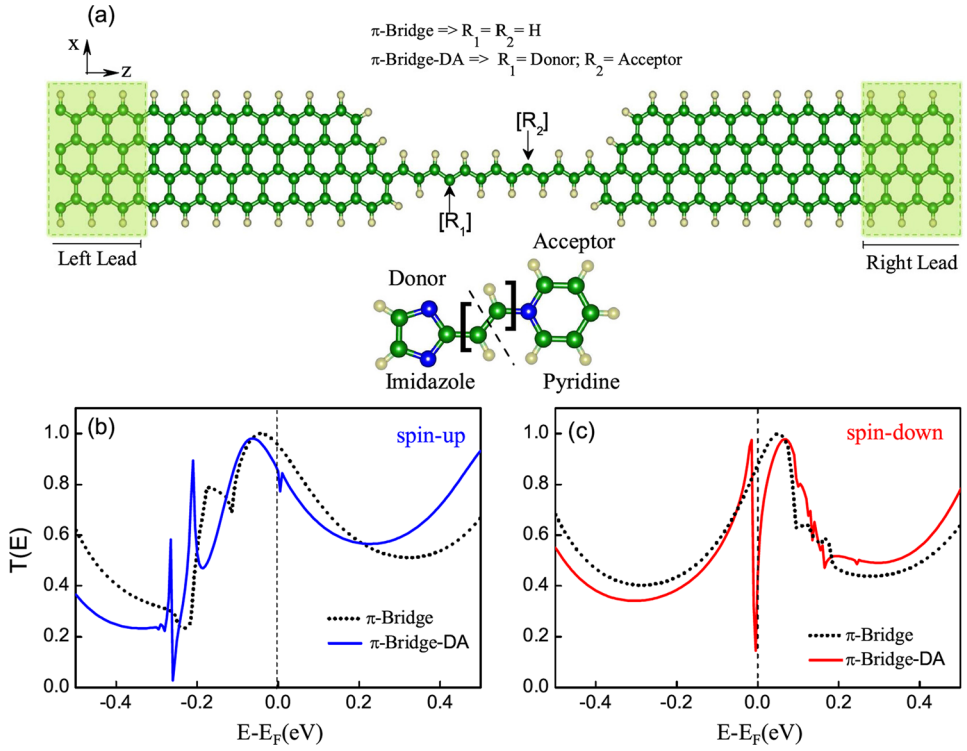

Figure 1. (a) Schematic of the two-probe structure studied in the electron transport calculations. The structures consist of ZGNR electrodes bridged by a polyacetylene chain. The shaded regions contain the semi-infinite left and right electrodes, which repeat to infinity to the left and right, respectively. The polyacetylene chain was studied in different scenarios: being passivated with hydrogen atoms (R_1 = R_2 = H), denoted π-bridge; or having donor (R_1 = imidazole) and acceptor (R_2 = pyridine) groups added at the positions shown, denoted π-bridge-DA. (b) and (c) Computed transmission spectra of the two systems described in (a) (dashed line: π-bridge, solid line: π-bridge-DA) for spin-up and spin-down, respectively. The atoms are colored as green for C, white for H, and blue for N.

conductances of molecular rods.[23] This interesting effect was then demonstrated in a molecular conductor, confirming that it is possible to control the current through a single molecule by chemical design.[24]

In this article, a junction consisting of ZGNR electrodes bridged by a polyacetylene carbon chain is investigated with electron and spin transport calculations. A similar molecular bridge connected to Au electrodes has been investigated with electron transport calculations by Yao et al.,[25] who found that the introduction of bridging groups to *cis*-polyacetylene can drastically affect the electron transport behavior by influencing the energy levels of frontier molecular orbitals and the extent of their spatial resolution. We have previously shown that attaching the polyacetylene chain to the ZGNRs in a para or meta configuration would result in very distinct electron transmission properties, and the para configuration yielded a more conductive system.[26] Therefore, the para configuration is utilized in this work. These transport properties are obtained with the nonequilibrium Green's function approach combined with density functional theory (NEGF-DFT). As stated above, ZGNR electrodes possess spin polarization along the edges, which results in a splitting of the spin-up and spin-down electron transport properties.[27] The addition of a donor group (imidazole) and an acceptor group (pyridine) to the polyacetylene chain leads to control over the transmission properties, introducing DQI. Finally, a gate voltage (V_g), which does not destroy the destructive interference, can be used to tune the electron transport properties such as the DQI, the overall conductance, and the spin filter efficiency.

COMPUTATIONAL DETAILS

The electron and spin transport properties of this system were investigated with the nonequilibrium Green's function approach combined with density functional theory (NEGF-DFT). This technique yields the transmission spectrum detailing the probability of an electron with a given energy of passing through the junction in a two-probe geometry, as shown in Figure 1a. The electronic structure and geometry optimizations were performed with density functional theory (DFT)[28,29] as implemented in the SIESTA code,[30] which employs a linear combination of atomic orbitals (LCAO) to expand the Kohn–Sham orbitals. The valence electronic orbitals of the systems were described using double-ζ polarized basis sets,[31] and norm-conserving Troullier–Martins pseudopotentials represented the core orbitals.[32] The local spin density approximation (LSDA)[33−35] was used since it adequately describes the antiferromagnetic/ferromagnetic ordering in carbon nanoribbons, which is very sensitive to the functional used.[36] A cutoff energy of 150 Ry was used, and in all cases, the relaxations were carried out until the force on each atom was less than 0.05 eV/Å. The Brillouin zone was sampled as a Monkhost–Pack grid[37] using 1 × 1 × 100 *k*-points.

The relaxed, minimum energy structure for the polyacetylene bridge case (π-bridge: R_1 = R_2 = H) is shown in Figure 1a. Along the polyacetylene chain, the C–H bond lengths were fairly uniform between 1.1 and 1.2 Å, and the C–C bond lengths were between 1.39 and 1.42 Å. When donor and acceptor groups were attached to the polyacetylene chain (π-bridge-DA: R_1 = imidazole, R_2 = pyridine), the C–H and C–C bond lengths within the polyacetylene chain were similar to the π-bridge case; the (C–C) bond length between the donor and the polyacetylene chain was 1.49 Å and between the acceptor and the polyacetylene chain was 1.45 Å. It turns out that the steric interactions of the donor and acceptor groups with the polyacetylene chain cause them to rotate out of the plane of the polyacetylene bridge system.

dx.doi.org/10.1021/ja508537n | J. Am. Chem. Soc. 2014, 136, 15065−15071

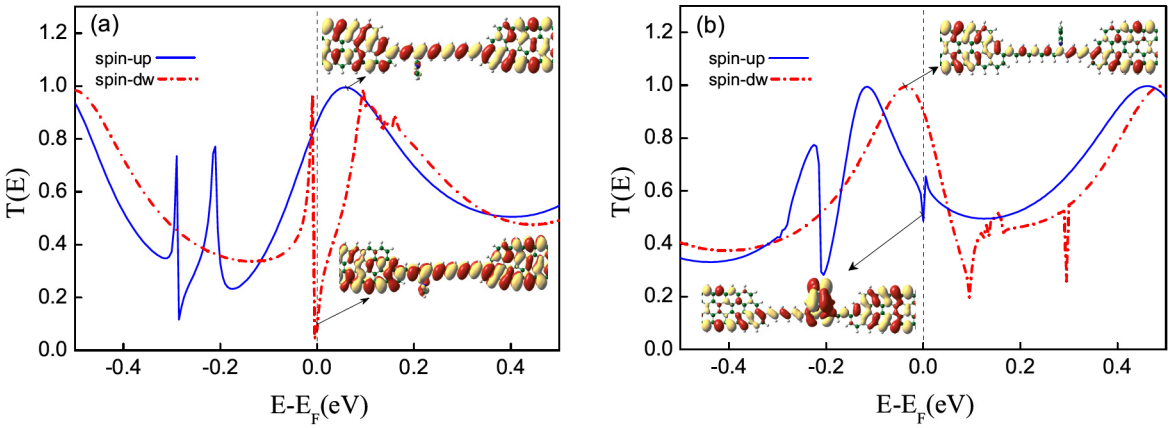

Figure 2. Transmission spectra for (a) π-bridge-D and (b) π-bridge-A systems. Spin-up is plotted in solid blue, and spin-down is plotted in dashed red. Scattering states corresponding to selected peaks and dips are included (isovalue = 0.02).

The electronic transport properties are obtained using the Nanodcal code,[38,39] which employs the nonequilibrium Green's function (NEGF) technique within the Keldysh formalism in combination with DFT.[40] This technique is applied to a two-probe system, as illustrated in Figure 1a. Note that in these calculations all atoms are described self-consistently at the same level of theory for the central region as well as the electrodes. This approach has been thoroughly described in the literature.[38,41−46]

To briefly summarize, the retarded Green's function is defined as,

$$G = (E^{+}S - H - \Sigma_{L}(E) - \Sigma_{R}(E))^{-1} \quad (1)$$

where $E^{+} = \lim_{\eta\to 0}[E + i\eta]$ is the energy plus an infinitesimal imaginary part $i\eta$. H is the Hamiltonian, and S is the corresponding overlap matrix obtained from a conventional DFT calculation on the central scattering region. $\Sigma_{L/R}$ are the self-energies that account for the effect of each electrode on the central scattering region. Each consists of two parts: the energy level shift is given by the real part as $\Delta_{L/R}(E) = \mathrm{Re}\Sigma_{L/R}(E)$, and the level broadening is given by the imaginary part:

$$\Gamma_{L/R}(E) = i(\Sigma_{L/R} - \Sigma_{L/R}^{\dagger}) \quad (2)$$

The Landauer−Büttiker transmission[47] probability can be calculated as the trace over the matrix product of the coupling matrices $\Gamma_{L/R,\sigma}$[48] and the $(G/G^{\dagger})$ Green's function of the central region. The transmission around the Fermi energy at zero bias is $[T_{\sigma}(E,V = 0)]$,

$$T_{\sigma}(E, V) = \mathrm{Tr}(\Gamma_{R,\sigma}G_{\sigma}\Gamma_{L,\sigma}G_{\sigma}^{\dagger}) \quad (3)$$

which represents the probability that an electron having spin σ and with a given energy E transmits from the left electrode, through the central region, into the right electrode.

The spin-polarized current versus voltage is obtained from

$$I_{\sigma}(E, V) = \frac{e}{\hbar}\int_{-\infty}^{+\infty} T_{\sigma}[f_{L}(E, \mu_{L}) - f_{R}(E, \mu_{R})]\mathrm{d}E \quad (4)$$

where the electrochemical potential difference between left and right electrodes is $eV = \mu_{L} - \mu_{R}$ and f is the Fermi distribution,

$$f_{L/R}(E, \mu) = \frac{1}{\exp[(E - \mu_{L/R})/kT] + 1} \quad (5)$$

The spin filter efficiency[49,50] (SFE) at the Fermi level is defined as

$$\mathrm{SFE} = \frac{|T_{up}(E_F) - T_{down}(E_F)|}{T_{up}(E_F) + T_{down}(E_F)} \quad (6)$$

and represents the excess transmission of one spin type over the other as a percentage of the total transmission. We calculated the SFE achieved at zero bias under different gate voltages for the π-bridge-DA system. The gate effect is simulated by setting a gate-induced electrostatic boundary condition for the Hartree potential when solving the Poisson equation in the NEGF-DFT self-consistent procedure. The density functional and basis set were the same in the NEGF-DFT calculations as those used for the structure relaxations.

RESULTS AND DISCUSSION

In the central region of the junction, the polyacetylene bridge is explored with and without donor/acceptor groups attached to the bridge (see Figure 1). Generally, π-conjugated organic molecules are good candidates for exhibiting magnetic order.[51] However, magnetic properties are not commonly found in pure organic molecules, and they are usually doped by a metal to possess magnetic characteristics.[49] In the system where the π bridge consists of a 13 carbon atom chain containing only H atoms (π-bridge case: $R_1 = R_2 = \mathrm{H}$), the transmission spectrum $T(E)$ shows broad peaks around the Fermi energy for spin-up and spin-down, as illustrated with the dashed lines in Figure 1b and c, respectively. The shape and position of these transmission peaks signify that such a junction would conduct electrons well at low bias. By adding imidazole as a donor group and pyridine as an acceptor group to the polyacetylene chain (π-bridge-DA system), the transmission exhibits a very small dip around the Fermi energy for spin-up (solid line in Figure 1b), while for spin-down (solid line in Figure 1c)), the transmission exhibits a sharp dip near the Fermi energy suggesting DQI. The calculations show that the transmission for the π-bridge is high ($T(E_F) \approx 1$) and is very sensitive to the addition of the donor and acceptor groups. When these side groups are added, the transmission has an impressive antiresonance dip that brings the value to almost $T(E_F) \approx 0$ for the spin-down case. It should be pointed out that the effect of DQI due to the addition of side groups has been previously described. For example, Papadopoulos et al. showed that the presence of fluorenone side groups on molecular wires results in Fano resonances close to the Fermi energy of those systems.[52]

In order to reveal the influence of the donor and acceptor groups on the DQI effect from Figure 1b and c, the influence of each group on the transmission is calculated separately. It is important to emphasize that the most relevant energy region for low-bias conductance is near E_F. Figure 2a shows the transmission for a polyacetylene chain bridging ZGNR electrodes with just an imidazole donor group added to the chain (π-bridge-D). For spin-up (solid blue line), the transmission has a large peak reaching a value of 1 at E = 0.05 eV. However, in the spin-down plot there is a large dip in

dx.doi.org/10.1021/ja508537n | J. Am. Chem. Soc. 2014, 136, 15065−15071

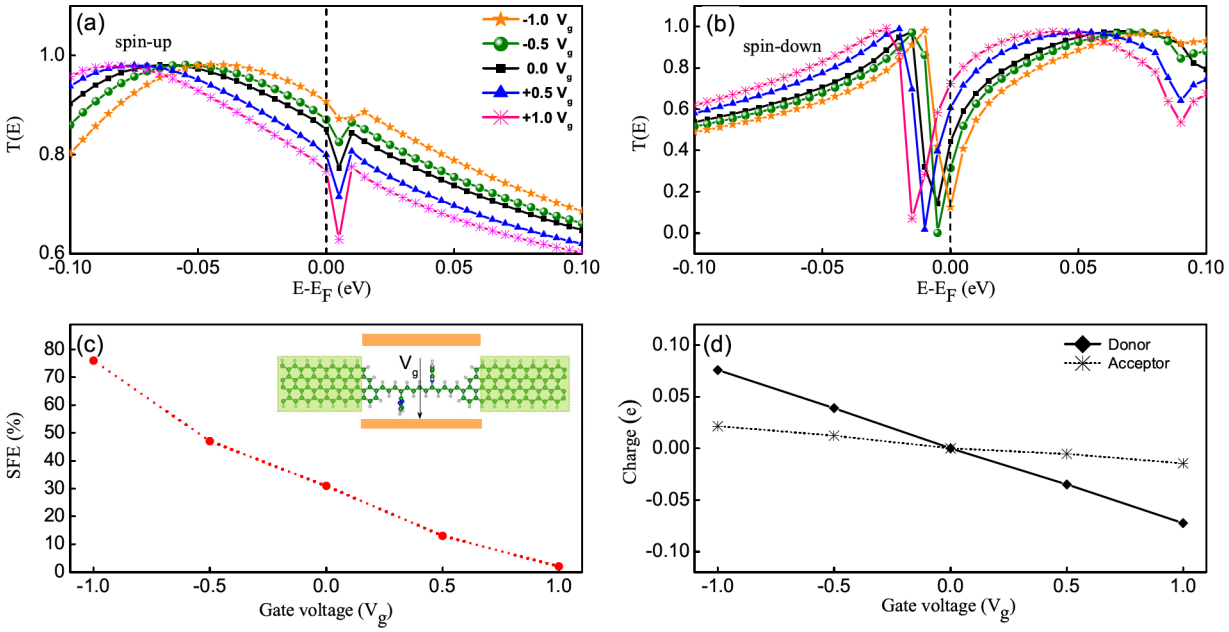

Figure 3. (a) Spin-up and (b) spin-down transmission under the influence of an external gate voltage (V_g). Note the scale of the axes: this is a close up of the transmission near E_F. (c) The SFE as a function of V_g. (d) The charge on the donor and acceptor groups (Mulliken distribution) under V_g.

transmission at the E_F corresponding to DQI. Analysis of the scattering states for these two scenarios (spin-up vs spin-down) can be very insightful. For spin-up, the scattering state at E = 0.05 eV (top right of Figure 2a) shows that there is no amplitude on the imidazole side group, such that it is unrecognized in terms of transmission at that energy and the transmission resembles that of the π-bridge system lacking a donor group. On the other hand, for spin-down, the scattering state at E_F shows amplitude on the donor side group, which results in a DQI effect and a sharp dip in transmission at that energy. This sort of DQI effect has been described previously as being due to antiresonances induced by side chains.[20]

Figure 2b shows the transmission spectrum for the polyacetylene chain bridging ZGNR electrodes with a pyridine acceptor group added to the chain (π-bridge-A). For this system, neither the spin-up transmission (solid blue plot) nor the spin-down transmission (dashed red plot) have a significant antiresonance at the E_F. The spin-up plot does show a small dip in transmission at E_F which is attributed to a small amount of DQI, also due to the presence of the side chain, the pyridine acceptor in this case. The scattering state corresponding to this transmission dip is illustrated at the bottom left of Figure 2b. Note that there is amplitude on the pyridine, but it does not contribute to a significant antiresonance in this case (the dip in transmission is quite small). For the spin-down case, the scattering state corresponding to the peak in transmission shows that there is no amplitude on the pyridine side group, which has no effect on the spin-down transmission at this energy (−0.03 eV).

This comparison demonstrates that DQI in the π-bridge-DA system can arise from either side group (donor or acceptor) for a given spin and energy. While both the donor and the acceptor groups result in antiresonance dips, the position in energy can be very different and depends on the chemistry of the side group. In fact, many other side groups would have similar antiresonance dips, and the position relative to the Fermi level could be tuned with judicious selection of the donor/acceptor molecule. In fact, this effect is often observed when side groups are added to a chain, as described by Hansen et al.[20] The donor group contributes to the large antiresonance dip at E_F for spin-down, while the acceptor group contributes to the small antiresonance dip at E_F for spin-up. With both of these two side groups, the transmission at E_F is dominated by DQI. Experimental and theoretical works have shown that DQI might be used to control the current through a molecular device.[24,53] However, it is very difficult to pinpoint the position of the antiresonance dip relative to the E_F and even more difficult to control it. This can be related to the position of the frontier molecular orbitals relative to the E_F of the electrodes when the junction is formed, which can also be dependent upon the dipole moment at the surface of the electrode (which is metal in most cases).[4] In practice, a gate voltage, V_g, may be used to shift the molecular levels relative to the E_F, thus bringing the molecular system into an open conduction regime. The gate voltage, V_g, controls the conducting channels and can turn on/off the molecular device. An example of such a system is described by Baratz et al., who showed that a gate can induce an intramolecular charge transfer in a molecular junction containing a donor/acceptor pair, resulting in conductance switching.[54] For this purpose, we are interested in controlling the DQI in the π-bridge-DA system upon the application V_g (along the x-direction in Figure 1a) ranging from −1.0 to +1.0 V.

Figure 3a and b shows the spin-up and spin-down transmission of the π-bridge-DA system under a gate voltage V_g. In our simulations, the gate region encompasses the entire central region, including the acceptor and donor molecules shown in the inset of Figure 3c. Therefore, all atoms in the central region are gated, and self-consistency is maintained.[55] Note that these spectra are close-ups of the transmission at E_F. For the spin-up transmission (panel a), the transmission spectrum shifts slightly with the V_g, going to more positive energies with more negative V_g. There is a small antiresonance dip at 0.005 eV, with the magnitude of the dip varying with V_g, but the energy remains constant. The antiresonance dip nearly disappears at V_g = −1.0 V and is largest at V_g = +1.0 V. Note

dx.doi.org/10.1021/ja508537n | J. Am. Chem. Soc. 2014, 136, 15065−15071

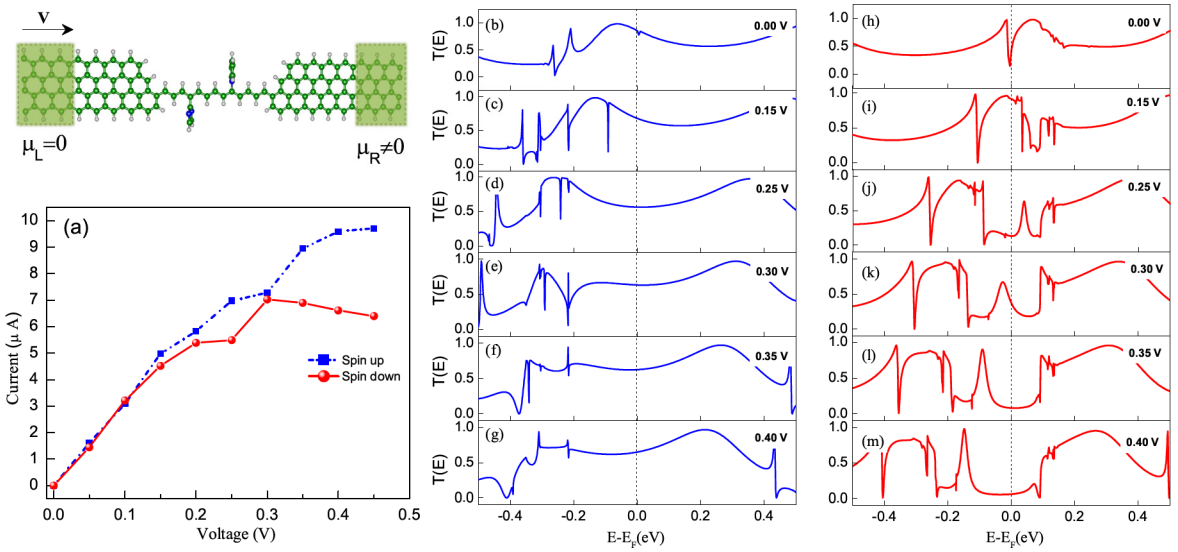

Figure 4. (a) Spin-up (dashed blue) and spin-down (solid red) current as a function of bias between left and right electrodes ($\mu_L = 0$ and $\mu_R \neq 0$ for the π-bridge-DA system (shown above panel a). (b–g) Spin-up and (h–m) spin-down transmission spectra at various biases.

the transmission scale, and that at all V_g values, the dip is relatively small and does not have a significant effect on the transmission at E_F. The different $T(E_F)$ values can be attributed to the shift in spectra under V_g. For the spin-down transmission (panel b), there is a similar shift in transmission spectra with V_g. However, in this case, the antiresonance dip shifts in energy but remains approximately the same size (drops down to ca. $T \approx 0.1$). In the spin-down case, the V_g can be used to bring the antiresonance dip into and out of alignment with the E_F, which results in a substantial difference in $T(E_F)$ ranging from 0.1 to 0.7. Note that the antiresonance should be located around the Fermi energy for this effect to be useful, but its position depends strongly on the coupling to the electrodes and is difficult to accurately predict. The problem is related to the alignment of molecular levels and to the molecule–electrode interface. In this work, this limitation is avoided by analyzing the effects of a gating voltage, which is applied externally. This work illustrates that the gate can be utilized to tune the antiresonance relative to the Fermi level.

Since the V_g has a large effect on the spin-down transmission, but a relatively smaller effect on the spin-up transmission, it could be utilized to control the spin filter efficiency (SFE) through the π-bridge-DA system. Figure 3c shows the value of SFE calculated with eq 6 as a function of V_g for this system. The maximum SFE is achieved at $V_g = -1.0$ V, where the spin-down antiresonance dip is aligned with the E_F and over 75% of the current has spin-up polarization. Figure 3d shows the (Mulliken) charge on the donor and acceptor groups as the V_g is varied. Note that there is very little change on the acceptor charge but a relatively large change on the donor group. Surprisingly, the change in charge on both the donor and acceptor group is of the same sign for a particular V_g, suggesting the charge is transferred from the polyacetylene chain or the ZGNR electrodes into the groups and not from one group to the other. We interpret this as a charge transfer into the molecules flowing from the electrodes through the π-bridge-DA.

The transmission spectra shown so far are for zero-bias conditions, and they are instructive in understanding the low-bias conductance properties of molecular devices. However, to understand how such devices will behave under finite source-drain bias, the NEGF-DFT approach can be employed to calculate the (spin-dependent) transmission and current when a bias is applied between the two ZGNR electrodes. Figure 4a shows the spin-up (dashed blue) and spin-down (solid red) current for various applied biases. The current for spin-up and spin-down increase uniformly until 0.1 V, beyond which there is an excess spin-up current. At 0.45 V there is a substantial difference between the two, with roughly 50% more spin-up current than spin-down current. For the spin-down case, there is a slight negative differential resistance (NDR) from 0.3 to 0.45 V. The NDR mechanism is characterized by a local maximum in the transmission with the bias voltage increase. Figure 4b–g shows the evolution of the spin-up transmission spectrum as the bias is increased. For the values plotted, the spin-up transmission peaks shift in energy due to the bias change, but there is substantial transmission near E_F in all cases with only small variations.[56] For this reason, the spin-up current increases relatively uniformly. Figure 4h–m shows the evolution of the spin-down transmission spectrum as the bias voltage is increased. Here, the DQI near E_F plays a role in the I–V characteristics. As can be seen from the transmission spectra, the transmission near E_F changes substantially with different bias voltages, causing weak NDR for the spin-down current. At low bias, there is substantial transmission near E_F, but this becomes suppressed at higher bias values due to the DQI in the spin-down π-bridge-DA system.

SUMMARY

The spin-transport properties of a polyacetylene chain bridging zigzag graphene nanoribbon (ZGNR) electrodes were investigated using the nonequilibrium Green's function technique combined with density functional theory. ZGNR electrodes with the width studied in this work possess an inherent spin-polarization along their edges, resulting in splitting of the spin-up and spin-down electronic properties of these devices. The addition of an imidazole donor group and a pyridine acceptor group to the polyacetylene chain caused destructive quantum interference features in the transmission spectra. The largest effect was due to the donor group, which causes a large antiresonance dip in the spin-down transmission spectrum right

dx.doi.org/10.1021/ja508537n | J. Am. Chem. Soc. 2014, 136, 15065–15071

at the E_F level of the ZGNR electrodes. By applying a gate voltage to the device, the energy antiresonance dip may be controlled to bring it into and out of alignment with the E_F—leading to a control of the spin filter efficiency of this system ranging from 0% to over 75%. Finally, the calculated $I-V$ properties of the π-bridge-DA system show that the spin-up current increases fairly uniformly with applied (source−drain) bias, while the spin-down current exhibits slight negative differential resistance due to the destructive quantum interference. These results outline some possibilities for controlling the spin-transport properties in spintronic devices with the application of a gate voltage and by exploiting quantum interference properties of molecular devices.

■ ASSOCIATED CONTENT

Supporting Information

Scattering state analysis of the antiresonance dip at −0.1 eV in Figure 4c and atomic coordinates and total energies of all structures used in the work. This material is available free of charge via the Internet at http://pubs.acs.org.

■ AUTHOR INFORMATION

Corresponding Authors

saraivaa@physics.mcgill.ca
manuel.smeu@nothwestern.edu

Notes

The authors declare no competing financial interest.

■ ACKNOWLEDGMENTS

A.S.-S. acknowledges the Brazilian agency CNPq for the postdoctoral program fellowship (process 246199/2012-1), CENAPAD-SP, CLUMEQ, CalculQuebec, and Compute-Canada for computational support. M.S. thanks FRQNT for financial support. L.Z. thanks CLUMEQ, CalculQuebec, and Compute-Canada for computation facilities. A.G.S.F. thanks FUNCAP through PRONEX grant. H.G. thanks NSERC Canada. M.A.R. thanks the chemistry division of the NSF for support (CHE-1058896).

■ REFERENCES

(1) Aviram, A.; Ratner, M. A. *Chem. Phys. Lett.* **1974**, *29*, 277−283.
(2) Žutić, I.; Fabian, J.; Sarma, S. *Rev. Mod. Phys.* **2004**, *76*, 323−410.
(3) Basch, H.; Cohen, R.; Ratner, M. *Nano Lett.* **2005**, *5*, 1668−1675.
(4) Hofmann, O. T.; Egger, D. A.; Zojer, E. *Nano Lett.* **2010**, *10*, 4369−4374.
(5) Frei, M.; Aradhya, S. V.; Koentopp, M.; Hybertsen, M. S.; Venkataraman, L. *Nano Lett.* **2011**, *11*, 1518−1523.
(6) Li, G.; Tamblyn, I.; Cooper, V. R.; Gao, H.-J.; Neaton, J. B. *Phys. Rev. B* **2012**, *85*, 121409.
(7) Guo, X.; Small, J. P.; Klare, J. E.; Wang, Y.; Purewal, M. S.; Tam, I. W.; Hong, B. H.; Caldwell, R.; Huang, L.; O'Brien, S.; Yan, J.; Breslow, R.; Wind, S. J.; Hone, J.; Kim, P.; Nuckolls, C. *Science* **2006**, *311*, 356−359.
(8) Ke, S.-H.; Baranger, H. U.; Yang, W. *Phys. Rev. Lett.* **2007**, *99*, 146802.
(9) Cao, Y.; Liu, S.; Shen, Q.; Yan, K.; Li, P.; Xu, J.; Yu, D.; Steigerwald, M. L.; Nuckolls, C.; Liu, Z.; Guo, X. *Adv. Funct. Mater.* **2009**, *19*, 2743−2748.
(10) Prins, F.; Barreiro, A.; Ruitenberg, J. W.; Seldenthuis, J. S.; Aliaga-Alcalde, N.; Vandersypen, L. M. K.; van der Zant, H. S. J. *Nano Lett.* **2011**, *11*, 4607−4611.
(11) Kim, K.; Coh, S.; Kisielowski, C.; Crommie, M. F.; Louie, S. G.; Cohen, M. L.; Zettl, A. *Nat. Commun.* **2013**, *4*, 2723.
(12) Son, Y.-W.; Cohen, M. L.; Louie, S. G. *Nature* **2006**, *444*, 347−349.
(13) Botello-Méndez, A. R.; Cruz-Silva, E.; Romo-Herrera, J. M.; López-Uras, F.; Terrones, M.; Sumpter, B. G.; Terrones, H.; Charlier, J.-C.; Meunier, V. *Nano Lett.* **2011**, *11*, 3058−3064.
(14) Robertson, A. W.; Warner, J. H. *Nanoscale* **2013**, *5*, 4079−4093.
(15) Chuvilin, A.; Meyer, J. C.; Algara-Siller, G.; Kaiser, U. *New J. Phys.* **2009**, *11*, 083019.
(16) Zeng, M. G.; Shen, L.; Cai, Y. Q.; Sha, Z. D.; Feng, Y. P. *Appl. Phys. Lett.* **2010**, *96*, 042104.
(17) Li, Y. W.; Yao, J. H.; Zhu, X. D.; Liu, C. J.; Jiang, J. Q.; Deng, X. S. *eXPRESS Polym. Lett.* **2009**, *3*, 684−691.
(18) Cardamone, D. M.; Stafford, C. A.; Mazumdar, S. *Nano Lett.* **2006**, *6*, 2422−2426.
(19) Herrmann, C.; Solomon, G. C.; Ratner, M. A. *J. Am. Chem. Soc.* **2010**, *132*, 3682−3684.
(20) Hansen, T.; Solomon, G. C.; Andrews, D. Q.; Ratner, M. A. *J. Chem. Phys.* **2009**, *131*, 194704.
(21) Ke, S.-H.; Yang, W.; Baranger, H. U. *Nano Lett.* **2008**, *8*, 3257−3261.
(22) Donarini, A.; Begemann, G.; Grifoni, M. *Nano Lett.* **2009**, *9*, 2897−2902.
(23) Hong, W.; Valkenier, H.; Mészáros, G.; Manrique, D. Z.; Mishchenko, A.; Putz, A.; Garca, P. M.; Lambert, C. J.; Hummelen, J. C.; Wandlowski, T. *Beilstein J. Nanotechnol.* **2011**, *2*, 699−713.
(24) Guédon, C. M.; Valkenier, H.; Markussen, T.; Thygesen, K. S.; Hummelen, J. C.; van der Molen, S. J. *Nat. Nanotechnol.* **2012**, *7*, 305−309.
(25) Yao, J.; Li, Y.; Zou, Z.; Yang, J.; Yin, Z. *Physica B* **2011**, *406*, 3969−3974.
(26) Saraiva-Souza, A.; Smeu, M.; Terrones, H.; Souza Filho, A. G.; Ratner, M. A. *J. Phys. Chem. C* **2013**, *117*, 21178−21185.
(27) Note that, while spin-up and spin-down are arbitrarily assigned, the important point is that there is a distinct difference between the two spin types.
(28) Kohn, W.; Sham, L. *Phys. Rev.* **1965**, *140*, A1133−A1138.
(29) Hohenberg, P.; Kohn, W. *Phys. Rev.* **1964**, *136*, B864−B871.
(30) Soler, J. M.; Artacho, E.; Gale, J. D.; Garcia, A.; Junquera, J.; Ordejon, P.; Sanchez-Portal, D. *J. Phys.: Condens. Matter* **2002**, *14*, 2745−2779.
(31) Junquera, J.; Paz, O.; Sánchez-Portal, D.; Artacho, E. *Phys. Rev. B* **2001**, *64*, 235111.
(32) Troullier, N.; Martins, J. *Phys. Rev. B* **1991**, *43*, 1993−2006.
(33) von Barth, U.; Hedin, L. *J. Phys. C: Solid State Phys.* **1972**, *5*, 1629−1642.
(34) Gunnarsson, O.; Lundqvist, B. *Phys. Rev. B* **1976**, *13*, 4274−4298.
(35) Rajagopal, A. *J. Phys. C: Solid State Phys.* **1978**, *11*, L943−L948.
(36) Rudberg, E.; Salek, P.; Luo, Y. *Nano Lett.* **2007**, *7*, 2211−2213.
(37) Monkhorst, H. J.; Pack, J. D. *Phys. Rev. B* **1976**, *13*, 5188−5192.
(38) Taylor, J.; Guo, H.; Wang, J. *Phys. Rev. B* **2001**, *63*, 245407.
(39) Waldron, D.; Haney, P.; Larade, B.; MacDonald, A.; Guo, H. *Phys. Rev. Lett.* **2006**, *96*, 166804.
(40) Datta, S. *Superlattices Microstruct.* **2000**, *28*, 253−278.
(41) Yoshizawa, K.; Tada, T.; Staykov, A. *J. Am. Chem. Soc.* **2008**, *130*, 9406−9413.
(42) Deng, W.-Q.; Muller, R. P.; Goddard, W. A., III. *J. Am. Chem. Soc.* **2004**, *126*, 13562−13563.
(43) Shen, L.; Zeng, M.; Yang, S.-W.; Zhang, C.; Wang, X.; Feng, Y. *J. Am. Chem. Soc.* **2010**, *132*, 11481−11486.
(44) Ie, Y.; Hirose, T.; Nakamura, H.; Kiguchi, M.; Takagi, N.; Kawai, M.; Aso, Y. *J. Am. Chem. Soc.* **2011**, *133*, 3014−3022.
(45) Yeganeh, S.; Galperin, M.; Ratner, M. A. *J. Am. Chem. Soc.* **2007**, *129*, 13313−13320.
(46) Aravena, D.; Ruiz, E. *J. Am. Chem. Soc.* **2012**, *134*, 777−779.
(47) Datta, S. *Electronic Transport in Mesoscopic Systems*; Cambridge studies in semiconductor physics and microelectronic engineering; Cambridge University Press: New York, 1997.

(48) Lopez Sancho, M.; Lopez Sancho, J.; Rubio, J. *J. Phys. F: Met. Phys.* **1984**, *14*, 1205−1215.
(49) Shen, X.; Sun, L.; Benassi, E.; Shen, Z.; Zhao, X.; Sanvito, S.; Hou, S. *J. Chem. Phys.* **2010**, *132*, 054703.
(50) Wu, J.-C.; Wang, X.-F.; Zhou, L.; Da, H.-X.; Lim, K. H.; Yang, S.-W.; Li, Z.-Y. *J. Phys. Chem. C* **2009**, *113*, 7913−7916.
(51) Korshak, Y. V.; Medvedeva, T. V.; Ovchinnikov, A.; Spector, V. N. *Nature* **1987**, *326*, 370−372.
(52) Papadopoulos, T. A.; Grace, I. M.; Lambert, C. J. *Phys. Rev. B* **2006**, *74*, 193306.
(53) Arroyo, C. R.; Tarkuc, S.; Frisenda, R.; Seldenthuis, J. S.; Woerde, C. H. M.; Eelkema, R.; Grozema, F. C.; van der Zant, H. S. J. *Angew. Chem., Int. Ed.* **2013**, *52*, 3152−3155.
(54) Baratz, A.; Baer, R. *J. Phys. Chem. Lett.* **2012**, *3*, 498−502.
(55) The choice of the gated region can affect the quantitative results, so the region needs to be large enough to include sufficient electrode buffer layers in order to screen both the molecular junction and the gate from the electrodes.
(56) An in-depth analysis for one of these features from Figure 4c is provided in the Supporting Information.